

Model-based sensitivity analysis of incoherent effects on microwave radar observations of precipitation media

G. Ferrauto¹, F.S. Marzano^{1,2}, and G. Vulpiani^{1,2}

¹Dipartimento di Ingegneria Elettrica, University of L'Aquila, Italy

²Centro di Eccellenza CETEMPS, University of L'Aquila, Italy

Abstract. Precipitation media are characterized by hydrometeor distribution in a liquid, melting or ice phase. Their absorption and scattering properties can give rise to incoherent effects on the radar echo, mainly due to the angular scattering recovery. An approach to model the radar response in these conditions is to resort to the generalized radar equation, including incoherent effects. The generalized radar equation can be derived from the radiative transfer theory and its solution is not straightforward as it takes an integro-differential form. Within this context, we propose a fast, fairly accurate analytical algorithm to simulate the radar response in presence of a slab of rainfall or hail, characterized by a given precipitation rate. The solution is based on the expansion of the specific intensity in terms of Legendre polynomials, truncated to the first order. Accuracy of the analytical solution is evaluated against available numerical methods. Numerical results are compared to those obtained by using the classical radar equation for ground-based and space-based radars at frequency from C to Ka band. Incoherent effects are shown to apparently increase the received power and to be sensitive to the observation frequency and volumetric albedo.

1 Introduction

The radar equation in an attenuating medium, as generally stated, takes into account single scattering, due to raindrops, weighted by the path attenuation from the considered range gate to the radar antenna (Sauvageot, 1992). However, for intense to heavy rainfall, the albedo of precipitating ice and liquid hydrometeors can be significant at frequencies of 10 GHz or above (Marzano et al., 1994). This means that multiple scattering effects can play a relevant role in determining the radar received power (Ito et al., 1995). Disregarding this multiply scattered radiation in the formulation of the radar forward problem could affect the accuracy of both the rang-

ing and estimate of rainfall rate profile. In particular, neglecting the multiple scattering effects due to intense rainfall could lead to an overestimation of rain rate.

The objective of this work is to evaluate the possible impact of the rainfall incoherent backscattering upon the radar response in the 5 to 35 GHz frequency range through a numerical investigation based on the generalized radar equation, derived from the radiative transfer theory. Within this context a fast, fairly accurate analytical algorithm is proposed to simulate the radar response in presence of a slab of rainfall or hail, characterized by a given precipitation rate. The effects of precipitation multiple scattering are evaluated at various attenuating frequencies and for nadir observations.

The concept of radar apparent reflectivity in multiple scattering media and the definition of generalized radar equation are introduced in Sect. 2. Section 3 illustrates the radar propagation model derived from the radiative transfer theory. Numerical results are shown and discussed in Sect. 4 in terms of the observed apparent reflectivity for a simple rain-slab model.

2 Radar reflectivity in multiple scattering media

The meteorological radar equation in an attenuating medium relates the mean received power $\langle P_R(r) \rangle$, obtained from the average of back-scattered pulses within a given range gate defining the scattering volume, to the transmitted power P_T , as follows (Sauvageot, 1992):

$$\langle P_R(r) \rangle = C P_T Z_e(r) \frac{L^2(r)}{r^2} \quad (1)$$

where C is the radar instrumental constant, Z_e is the equivalent reflectivity factor of the range-gated scattering volume, $L(r)$ is the attenuation factor, and r is the distance between the radar antenna and the considered range gate. Only the scalar form of the radar equation is analyzed here, even though (1) might be easily extended to polarimetric measurements. The one-way attenuation factor $L(r)$, indicating the

Correspondence to: G. Ferrauto
(ferrauto@ing.univaq.it)

total attenuation between the radar and the considered range gate, is given by:

$$L(r) = e^{-\tau(r)} = e^{-A(r)/4.343} = e^{-\int_0^r k_e(r') dr'} \quad (2)$$

where k_e is the range-dependent volumetric extinction coefficient and τ is the optical thickness such that the one-way path attenuation is $A(r) = 4.343 \tau(r)$ (in dB). Even though in the radar literature τ generally indicates the pulse duration, here we have adopted the radiative transfer notation (Ishimaru, 1978; Tsang et al., 1985).

The radar instrumental constant C basically takes into account the antenna gain, the beamwidth, the pulse duration, the guidance losses, and the radar wavelength. Indeed, the constant C includes also a medium refractive-index term, which is usually assumed constant. Other factors due to the implemented digital signal processing, as the matched filtering, can be also inserted in C . Notice that the range gate is generally supposed to be completely filled by the scattering volume, unless non-uniform beam filling corrections are considered.

The volumetric equivalent (effective) reflectivity factor Z_e can be related to the backscattering properties of the precipitation volume by means of (Ishimaru, 1978):

$$Z_e = \frac{\lambda^4}{\pi^5 |K|^2} \eta_e = \frac{\lambda^4}{\pi^5 |K|^2} p(\Omega_s = \pi) k_s \quad (3)$$

where λ is the radar wavelength, K is the so-called dielectric factor (equal to 0.93 for water drops), η_e is the volumetric equivalent radar reflectivity, $p(\Omega_s = \pi)$ is the volumetric scattering phase function computed in the backward direction (i.e., for the scattering solid angle Ω_s equal to π), and k_s is the volumetric scattering coefficient.

The classical radar equation is derived under the assumption of single-scattering conditions and can include path attenuation, as shown by (1). However, in general conditions of multiple scattering, we expect the mean received power $\langle P_R(r) \rangle_{MS}$ to be higher with respect to $\langle P_R(r) \rangle$. If F_T [$\text{W m}^{-2} \text{Hz}^{-1}$] is the power flux density related to the transmitted power P_T and $\langle I_R(r) \rangle_{MS}$ [$\text{W m}^{-2} \text{sr}^{-1} \text{Hz}^{-1}$] is the received mean specific intensity due to the range gate at distance r , the volumetric apparent radar reflectivity η_{aMS} at range r and in the direction Ω_g can be defined in a way analogous to the surface scattering coefficient σ^0 (Tsang et al., 1985), that is:

$$\eta_{aMS}(\Omega, r) = \frac{4\pi \langle I_R(\Omega, r) \rangle_{MS}}{\Delta r F_T(\Omega, r)} \quad (4)$$

being $\Delta r = c\Delta t/2$ the range resolution, with Δt the pulse width and c the light velocity.

In the narrow-beam approximation, the multiply scattered received power $\langle P_R(r) \rangle_{MS}$ can be expressed as (Marzano et al., 2003):

$$\langle P_R(r) \rangle_{MS} \cong C \frac{P_T Z_{aMS}(\Omega_0, r)}{r^2} \quad (5)$$

where Z_{aMS} is the apparent reflectivity factor at range r in the radar beam Ω_0 direction.

Obviously, in analogy to (3), the apparent reflectivity factor Z_{aMS} can be expressed through the apparent radar reflectivity η_{aMS} :

$$Z_{aMS}(\Omega_0, r) = \frac{\lambda^4}{\pi^5 |K|^2} \eta_{aMS}(\Omega_0, r) \quad (6)$$

The generalized radar Eq. (5) can be simplified when considering only first-order scattering phenomena by introducing the first-order scattering apparent reflectivity factor Z_{aFS} . As a special case of (6), we can define Z_{aFS} as:

$$Z_{aFS}(\Omega_0, r) = \frac{\lambda^4}{\pi^5 |K|^2} \frac{4\pi \langle I_R(\Omega_0, r) \rangle_{FS}}{\Delta r F_T(\Omega_0, r)} \quad (7)$$

where $\langle I_R(\Omega_0, r) \rangle_{FS}$ is the received specific intensity in the first-order scattering approximation. From the radiative transfer theory, it can be demonstrated that (Ishimaru, 1978; Tsang et al., 1985):

$$Z_{aFS}(\Omega_0, r) \cong Z_e(r) L^2(r) \quad (8)$$

The above equivalence maintains its validity until the attenuation within the range bin centered at r becomes significant. It is worth mentioning that, by inserting (8) in place of Z_{aMS} in (5), we re-obtain the classical radar equation given by (1).

3 Radar response model for multiple scattering media

The generalized radar equation, derived from the radiative transfer theory in the previous section, takes into account both coherent and incoherent effects. However, its exact solution is not straightforward, since the computation of $\langle I_R(r) \rangle_{MS}$ requires the resolution of an integro-differential equation. So, a fast, simple, fairly accurate analytical algorithm is proposed to simulate the radar response in presence of a slab of rainfall or hail.

3.1 Description of the model

The transfer of unpolarized monochromatic radiation in a plane-parallel homogeneous random medium is regulated by the integro-differential radiative transfer equation, or RTE (Sobolev, 1962; Ishimaru, 1978):

$$\mu \frac{dI(\tau, \mu, \phi)}{d\tau} = -I(\tau, \mu, \phi) + J(\tau, \mu, \phi), \quad (9)$$

being $I(\tau, \mu, \phi)$ the diffuse specific intensity (or radiance) at the optical depth τ in the direction $\Omega = (\mu, \phi)$ and $J(\tau, \mu, \phi)$ the source function, given by

$$J(\tau, \mu, \phi) = \frac{\omega}{4\pi} \int_0^{2\pi} \int_{-1}^1 p(\mu, \phi; \mu', \phi') I(\tau, \mu', \phi') d\mu' d\phi' + \frac{\omega}{4\pi} F_0 p(\mu, \phi; \mu_0, \phi_0) e^{-\tau/\mu_0}. \quad (10)$$

The first term of J is sometimes referred to as the multiple scattering source, while the second term represents the coherent contribution due to a collimated incident source along the

direction (μ_0, ϕ_0) . Thermal emission is assumed to be negligible with respect to the incident beam (Ishimaru, 1978).

The notation in the above equations is in accordance with a spherical coordinates system:

- θ is the zenith angle, defined to be less than 90° if $z > 0$ and larger than 90° if $z < 0$;
- $\mu = \cos\theta$, is positive if $z > 0$ and negative if $z < 0$;
- ϕ is the azimuth angle;
- ω is the single scattering albedo;
- τ is the optical thickness of the medium at height z ;
- μ_0 is the cosine of the direct radiation zenith angle θ_0 ;
- ϕ_0 is the azimuth angle of the incident (direct) radiation;
- F_0 is the power flux density, or irradiance, of the incident (direct) radiation.

The zenith opacity at height z can be related to the volumetric extinction coefficient $k_e(z)$ as follows:

$$\tau = \int_0^z k_e(z') dz', \quad (11)$$

where τ is allowed to vary in the range $[0, \tau_s]$, being τ_s the total optical thickness of the scattering medium.

For brevity, the dependence on the wavelength is omitted being, in a way, implicitly included in the medium optical parameters τ and ω and in p .

As already indicated, $p(\mu, \phi; \mu', \phi')$ is the so called scattering phase function (normalized to 4π), defining the intensity of a radiation incident at direction $\Omega' = (\mu', \phi')$ being scattered into direction $\Omega = (\mu, \phi)$.

The solution of RTE is based on the expansion of the specific intensity in terms of Legendre polynomials, truncated to the first order:

$$I(\tau, \mu, \phi) = I_0(\tau, \mu) + I_1(\tau, \mu) \cos \phi, \quad (12)$$

where the functions $I_0(\tau, \mu)$ and $I_1(\tau, \mu)$ are approximated in accordance with the Eddington approach (Shettle and Weinman, 1970):

$$I_0(\tau, \mu) = I_{00}(\tau) + \mu I_{01}(\tau), \quad (13a)$$

$$I_1(\tau, \mu) = I_{10}(\tau) + \mu I_{11}(\tau). \quad (13b)$$

The phase function is also approximated by a Legendre polynomials series truncated to the first order and is characterized by its asymmetry factor g , that defines the shape of the diffraction peak (Shettle and Weinman, 1970; Xiang et al., 1994).

Under these simplifying assumptions, the series expansion terms in (13) are given by:

$$I_{00}(\tau) = C_{01}e^{-k_0\tau} + C_{02}e^{k_0\tau} - \alpha_0 e^{-\tau/\mu_0}, \quad (14a)$$

$$I_{01}(\tau) = m_0 (C_{01}e^{-k_0\tau} - C_{02}e^{k_0\tau}) - \beta_0 e^{-\tau/\mu_0}, \quad (14b)$$

$$I_{10}(\tau) = m_1 (C_{11}e^{-k_1\tau} - C_{12}e^{k_1\tau}) - \beta_1 e^{-\tau/\mu_0}, \quad (14c)$$

$$I_{11}(\tau) = C_{11}e^{-k_1\tau} + C_{12}e^{k_1\tau} - \alpha_1 e^{-\tau/\mu_0}, \quad (14d)$$

where

$$k_0 = \sqrt{3(1-\omega)(1-g\omega)}; \quad (15a)$$

$$m_0 = \sqrt{\frac{3(1-\omega)}{1-g\omega}}; \quad (15b)$$

$$\alpha_0 = \frac{3\omega}{4\pi} F_0 \mu_0^2 \frac{1+g(1-\omega)}{1-k_0^2 \mu_0^2}; \quad (15c)$$

$$\beta_0 = \frac{3\omega}{4\pi} F_0 \mu_0 \frac{1+3g(1-\omega)\mu_0^2}{1-k_0^2 \mu_0^2}; \quad (15d)$$

$$k_1 = \sqrt{3\left(1 - \frac{3\pi^2}{32}g\omega\right)}; \quad (15e)$$

$$m_1 = \frac{1}{k_1}; \quad (15f)$$

$$\alpha_1 = \frac{\frac{9}{16}\omega\mu_0 F_0 g \sqrt{1-\mu_0^2}}{1-\mu_0^2 k_1^2}; \quad (15g)$$

$$\beta_1 = \frac{\frac{9}{16}\omega\mu_0^2 F_0 g \sqrt{1-\mu_0^2}}{1-\mu_0^2 k_1^2}. \quad (15h)$$

The integration constants C_{01} , C_{02} , C_{11} and C_{12} in (14) can be computed by imposing the following boundary conditions, which state diffuse radiance is only generated within the scattering medium with optical thickness τ_s :

$$I(\tau = 0, \mu, \phi) = 0 \quad (16a)$$

$$I(\tau = \tau_s, \mu, \phi) = 0 \quad (16b)$$

The mean specific intensity reflected by the homogeneous layer can be simply calculated by (12) at the height $z=0$ (i.e. $\tau=0$) and considering the backward direction $\Omega_0 = (-\mu, \phi)$.

$$\begin{aligned} < I_R(\Omega_0) >_{MS} = C_{01} + C_{02} - \alpha_0 - \mu (m_0 C_{01} - m_0 C_{02} - \beta_0) \\ &+ [m_1 C_{11} - m_1 C_{12} - \beta_1 - \mu (C_{11} + C_{12} - \alpha_1)] \cos \phi. \end{aligned} \quad (17)$$

Above relation allows us to rapidly evaluate multiple scattering effects produced by a generic homogeneous scattering media. In particular, it can be used in a profitable way, together with the generalized radar Eq. (5), to quantify incoherent effects on the radar echo. However, accuracy of this fast analytical algorithm, that simulates the radar response in multiple scattering media, first need to be evaluated against more precise numerical methods of solution of RTE.

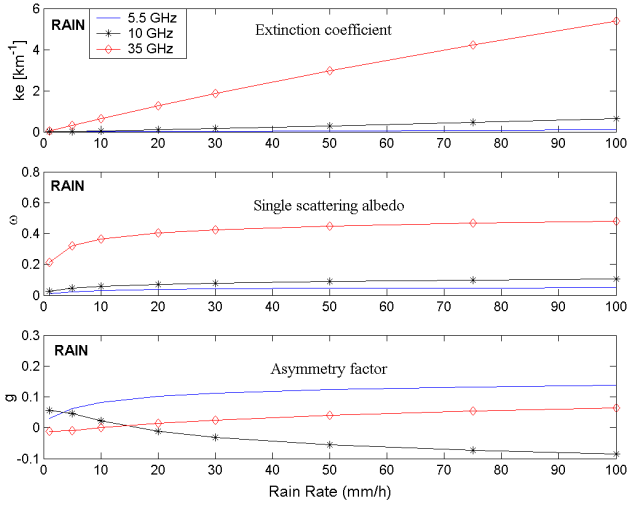


Fig. 1. Optical parameters simulated for a slab of rainfall at 3 different frequencies (5.5 GHz, 10 GHz and 35 GHz).

3.2 Validation of the model

Validation of the described radar propagation model is carried out considering the response of simple slabs of rainfall or graupel with a thickness of 500 m, each characterized by a given precipitation rate. Response of this algorithm in terms of reflected mean specific intensity is compared to the Discrete-Ordinate model (DISORT), a numerical solution of the RTE that gives highly accurate results so to be usually considered as a reference (e.g. Xiang et al., 1994; Levoni et al., 2001; Smith et al., 2002).

This procedure first requires the simulation of single-scattering radar parameters associated both to the rain-slab and to the graupel-slab; these parameters are computed by means of the Mie theory (assumption of spherical hydrometeors). Numerical simulations are done for ground-based and space-based radars at 3 different frequencies in the C, X and Ka band, that is at 5.5 GHz, 10 GHz and 35 GHz. The Heyney-Greenstein approximation is assumed for the volumetric scattering phase function (Heyney and Greenstein, 1941), while Marshall-Palmer and Gunn-Marshall DSD are used, respectively, to describe water and ice particle distribution. The single scattering radar parameters simulated for rainfall and graupel are illustrated in Fig.1 and in Fig. 2, respectively. It can be easily noted that rain shows absorbing properties quite sensitive to the frequency and stronger with respect to the graupel; from the other side, graupel scattering shows a higher intensity and a low grade of isotropy if compared with rain scattering.

Optical parameters k_e , g and ω , determined in such a way, are used as an input of the proposed radar response algorithm. Without loss of generality, F_0 and ϕ_0 are set to 1. A preliminary analysis suggests to adopt a delta-transformation technique (Joseph et al., 1976; Wiscombe, 1977) and a first-order scattering correction (e.g. Nakajima and Tanaka, 1988; Xiang et al., 1994; Levoni et al., 2001), in order to

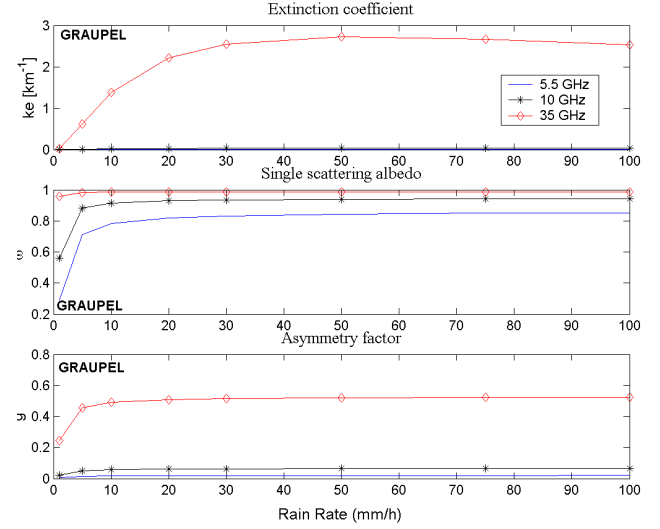


Fig. 2. Optical parameters simulated for a slab of graupel at 3 different frequencies (5.5 GHz, 10 GHz and 35 GHz).

Table 1. Observation geometry and number of test scenarios.

Observation Geometry									
$\mu = \cos\theta$									
ϕ									
0°	15°	30°	60°	90°	105°	120°	150°	165°	180°
Number of Test Scenarios: 60									

avoid unrealistic features produced by the approximated representation of the phase function; in this way, can be proved (27) produces better results (Marzano et al., 2003).

For a full validation, the wide series of observation geometries indicated in Tab.1 are considered; differences between the reflected intensities calculated by means of the proposed analytical algorithm and DISORT algorithm (Stamnes et al., 1988) are evaluated for each of the 60 test scenarios of Table 1 and are expressed as relative percentage errors. The mean value $\langle \epsilon \rangle$ and the standard deviation $\sigma(\epsilon)$ of these errors are also evaluated, respectively, in correspondence of each direction of observation established in Table 1.

Results of this analysis are represented in Fig. 3. The proposed analytical algorithm shows a very good accuracy for observation with C and X band radar systems. For an operating frequency of 35 GHz accuracy decays, but it maintains values that are acceptable; furthermore, it can be proved this accuracy decay is comparable with the loss of precision that the uncertainty in the knowledge of the optical parameters would produce.

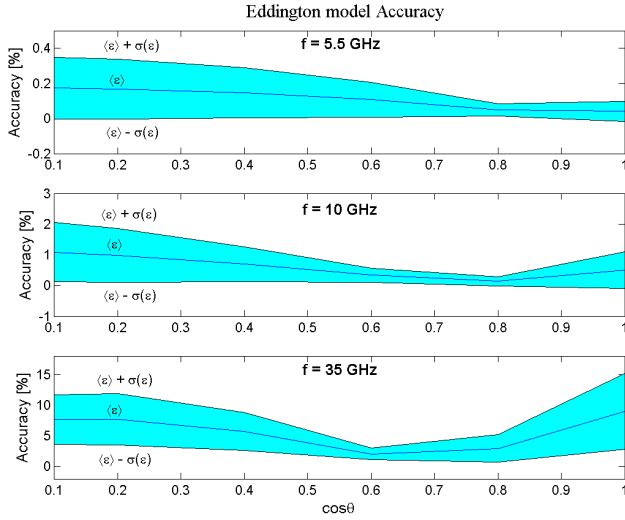


Fig. 3. Accuracy of the fast analytical radar response algorithm, measured by comparisons with DISORT model and illustrated in terms of relative percentage error.

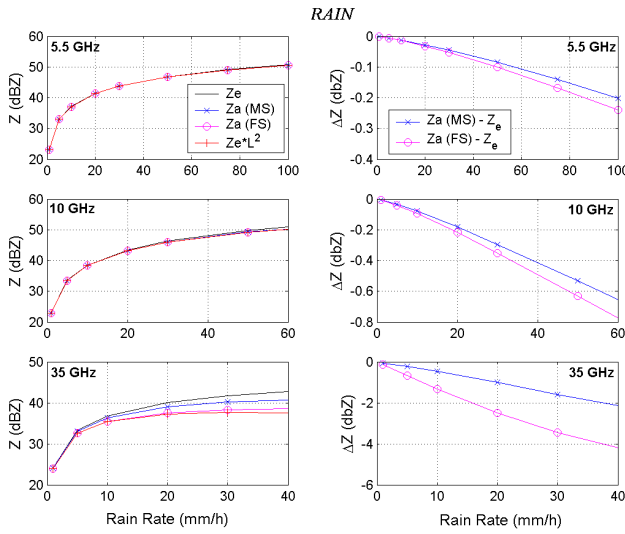


Fig. 4. Radar observation of a slab of rainfall at 3 different frequencies (5.5 GHz, 10 GHz and 35 GHz). Simulated radar response is illustrated in terms of apparent reflectivity factor Z_{aMS} , taking into account multiple scattering effects, compared with the effective reflectivity factor Z_e .

4 Numerical results

Numerical simulations are carried out for radar observations, at nadir, of single slabs of rainfall or graupel for the three frequency bands at 5.5 GHz, 10 GHz, and 35 GHz. Thickness of these layers is set to 500 m, that is the range resolution of radar systems having a pulse duration of $3.3 \mu s$; furthermore, for a given rain rate each slab is characterized by the optical parameters of Fig. 1 and 2.

Aim of this kind of analysis is to carry out a preliminary evaluation of the impact that incoherent effects, due to scat-

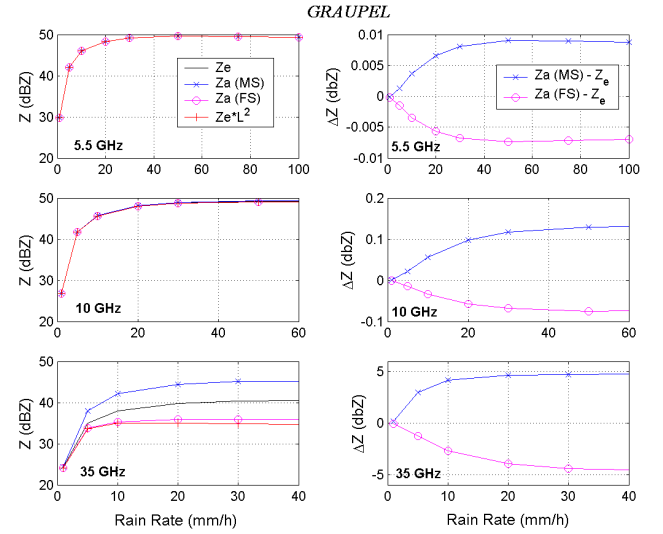


Fig. 5. Radar observation of a slab of graupel at 3 different frequencies (5.5 GHz, 10 GHz and 35 GHz). Simulated radar response is illustrated in terms of apparent reflectivity factor Z_{aMS} , taking into account multiple scattering effects, compared with the effective reflectivity factor Z_e .

tering phenomena within a range bin, can produce on the radar echo. Possible applications in reconstruction of reflectivity profile taking into account multiple scattering effects would require further considerations that are not the subject of this work.

Radar response is simulated by means the analytical algorithm illustrated in Sec.3: received mean specific intensity $\langle I_R(\Omega_o) \rangle_{MS}$ is evaluated by (27), to which delta-transformation and first-order scattering correction are applied; then, using (4) and (6) radiance is converted in the apparent reflectivity factor Z_{aMS} taking into account multiple scattering effects.

Effective reflectivity factor Z_e and first-order scattering apparent reflectivity factor Z_{aFS} are also calculated by means (3) and (7), respectively; notice that the received specific intensity $\langle I_R(\Omega_o, r) \rangle_{FS}$, taking into account only single scattering effects, is evaluated in the hypothesis of first-order scattering approximation of RTE (Liou, 1980; Tsang et al., 1985).

Figures 4 and 5 show both comparisons between the apparent and effective reflectivity factors at 5.5 GHz, 10 GHz, and 35 GHz for a slab of rainfall and graupel, respectively. At 5 and 10 GHz and for low rainfall rate all the reflectivities tend to coincide, as reasonable, since the atmospheric albedo and attenuation are negligible. As the frequency increases, shift between Z_e and Z_{aMS} becomes substantial: this is explained by an increasing of attenuation and scattering effects within the layer.

The difference between Z_{aMS} and Z_e gives a quantitative indication about attenuation and multiple scattering effects, while the difference between Z_{aFS} e Z_e only provides a measure of the attenuation effects, as deductible from (8). Notice

that the one-way attenuation factor L is measured as far as the center of the slab and that equivalence (8) slightly decay, at 35 GHz, for moderate to intense rainfall.

The previous figures prove that opposite effects are due to the combination of attenuation and multiple scattering. On one hand, attenuation is predominant for the single-scattering case and tends to reduce the equivalent reflectivity. On the other hand, multiple scattering tends to increase the single-scattering reflectivity, especially in the cloud regions characterized by large albedo, even though the effect of attenuation still reduces its values with respect to the equivalent reflectivity ones.

As expected, it holds for all the rainfall cases $Z_{aFS} < Z_{aMS} < Z_e$. Graupel scattering, instead, is so heavy that increasing in the single-scattering reflectivity due to multiple scattering completely cancels and turn over the attenuation effects: $Z_{aFS} < Z_e < Z_{aMS}$.

From a quantitative point of view, we can assert that radar observation of rainfall events at frequency of 10 GHz or above can be considerably influenced by incoherent effects just for moderate precipitation rate, with a difference between Z_{aMS} and Z_e amounting to $0.5 \div 1.5$ dBZ; amount of multiple scattering effects only, estimable by differences between Z_{aMS} and Z_{aFS} , is about $0.2 \div 1$ dBZ. C band radar systems, instead, show to be practically insensitive to multiple scattering effects.

Previous results suggest that, when multiple scattering is relevant, in the radar inverse problem the profile of the rain rate R should be derived from a power relationship using the estimated equivalent reflectivity Z_e instead of the apparent (measured) radar reflectivity Z_{aMS} . This means that an apparent attenuation factor (different from “true” single-scattering attenuation L), taking into account multiple scattering effects, should be evaluated for properly correcting Z_{aMS} . This might be accomplished, for instance, by an adaptive surface reference technique (Iguchi and Meneghini, 1994).

5 Summary and conclusions

A fast, fairly accurate analytical algorithm, based on the definition of generalized radar equation, was proposed to simulate the radar response when incoherent effects, due to scattering and absorbing media, become significant. The effects of precipitation multiple scattering were evaluated for radar observations, at nadir, of single slabs of rainfall or graupel for the three frequency bands at 5.5 GHz, 10 GHz, and 35 GHz. Thickness of each slab was set to 500 m, that is the most common range resolution of ground-based radar systems, so as to carry out a preliminary evaluation of the impact that incoherent effects, due to scattering phenomena within a range bin, can produce on the radar echo.

Numerical results showed that the difference between multiple-scattering reflectivity factor (Z_{aMS}) and the single-scattering one (Z_{aFS}) can give an indication of the multiple scattering effects, while the difference between Z_{aMS}

and the equivalent reflectivity factor Z_e also includes a measure of the attenuation effects. As expected, it holds for all the rainfall cases $Z_{aFS} < Z_{aMS} < Z_e$; if graupel scattering occurs, subsequent increasing in the single-scattering reflectivity could determine $Z_{aFS} < Z_e < Z_{aMS}$.

Radar observation of moderate to intense rainfall events at frequency of 10 GHz or above can be considerably influenced by incoherent effects, estimable in an increasing of about $0.2 \div 1$ dBZ on the measured reflectivity. Apparent attenuation factor should be properly evaluated in multiple scattering conditions to reconstruct equivalent reflectivity from apparent reflectivity measurements.

Acknowledgements. This work has been partially supported by Italian Space Agency (ASI), by Italian National Research Council (CNR) through GNDCI project and by Italian Ministry of Education, University and Research (MIUR).

References

- Heyney, L. G. and Greenstein, J. L.: Diffuse radiation in the galaxy, *Astrophys.*, 93, 70–83, 1941.
- Iguchi, T. and Meneghini, R.: Intercomparison of single-frequency methods for retrieving a vertical rain profile from an airborne or spaceborne radar data, *J. Atmos. Oceanic Tech.*, 11, 1507–1516, 1994.
- Ishimaru, A.: Wave propagation and scattering in random media, Vol. 1 and 2, Academic Press, New York, 1978.
- Ito, S., Oguchi, T., Iguchi, T., Kumagai, H., and Meneghini, R.: Depolarization of radar signals due to multiple scattering in rain, *IEEE Trans. Geosci. Remote Sens.*, 33, 1057–1062, 1995.
- Joseph, J. H., Wiscombe, W. J., and Weinman, J. A.: The Delta-Eddington Approximation for Radiative Flux Transfer, *Journal of the Atmospheric Sciences*, 33, 2452–2459, 1976.
- Levoni, C., Cattani, E., Cervino, M., Guzzi, R., and Di Nicolantonio, W.: Effectiveness of the MS-method for computation of the intensity field reflected by a multi-layer plane-parallel atmosphere, *J. Quant. Spectroscopy and Radiative Transfer*, 69, 5, 635–650, 2001.
- Liou, K. N.: An introduction to atmospheric radiation, Academic Press, New York (NY), 1980.
- Marzano, F. S., Mugnai, A., Smith, E. A., Xiang, X., Turk, J., and Vivekanandan, J.: Active and passive remote sensing of precipitating storms during CaPE. Part II: Intercomparison of precipitation retrievals from AMPR radiometer and CP-2 radar, *Meteor. Atmospheric Physics*, 54, 29–51, 1994.
- Marzano, F. S., Mugnai, A., Panegrossi, G., Pierdicca, N., Smith, E. A., and Turk, J.: Bayesian estimation of precipitating cloud parameters from combined measurements of spaceborne microwave radiometer and radar, *IEEE Trans. Geosci. Rem. Sens.*, 37, 596–613, 1999.
- Marzano, F. S., Roberti, L., Di Michele, S., Tassa, A., and Mugnai, A.: Modeling of apparent radar reflectivity due to convective clouds at attenuating wavelengths, *Radio Sci.*, 38, 1, 1002, doi:10.1029/2002RS002613, 2003.
- Nakajima, T. and Tanaka, M.: Algorithms for radiative intensity calculations in moderately thick atmospheres using a truncation approximation, *J. Quant. Spectroscopy and Radiative Transfer*, 69, 5, 635–650, 2001.

- Sauvageot, H.: Radar meteorology, Artech House, Norwood (MA), 1992.
- Shettle, E. P. and Weinman, J. A.: The Transfer of Solar Irradiance Through Inhomogeneous Turbid Atmospheres Evaluated by Edington's Approximation, *Journal of the Atmospheric Sciences*, 27, 1048–1055, 1970.
- Smith, E. A., Bauer, P., Marzano, F. S., Kummerow, C. D., McKague, D., Mugnai, A., and Panegrossi, G.: Intercomparison of microwave radiative transfer models for precipitating clouds, *IEEE Trans. Geosci. Remote Sens.*, 40, 541–549, 2002.
- Sobolev, V. V.: A Treatise on Radiative Transfer, D. Van Nostrand, 1962.
- Stamnes, K., Tsay, S. C., Wiscombe, W., and Jayaweera, K.: Numerically stable algorithm for discrete-ordinate-method radiative transfer in multiple scattering and emitting layered media, *Appl. Opt.*, 27, 12, 2502–2509, 1988.
- Tsang, L., Kong, J. A., and Shin, R. T.: Theory of microwave remote sensing, J. Wiley & Sons, New York (NY), 1985.
- Wiscombe, W. J.: The Delta-M Method: Rapid Yet Accurate Radiative Flux Calculations for Strongly Asymmetric Phase Functions, *Journal of the Atmospheric Sciences*, 34, 1408–1422, 1977.
- Xiang, X., Smith, E. A., and Justus, C. G.: A Rapid Radiative Transfer Model for Reflection of Solar Radiation, *J. Atm. Sci.*, 51, 13, 1978–1988, 1994.